Catal Lett (2008) 122:295–301
DOI 10.1007/s10562-007-9375-3

Hydrogen Production from Ethanol Steam Reforming Over Supported Cobalt Catalysts

Sean S.-Y. Lin · Do Heui Kim · Su Y. Ha

Received: 5 October 2007 / Accepted: 29 November 2007 / Published online: 11 December 2007

Abstract Hydrogen production was carried out via ethanol steam reforming over supported cobalt catalysts. Wet incipient impregnation method was used to support cobalt on ZrO_2, CeO_2 and $CeZrO_4$ followed by pre-reduction with H_2 up to 677 °C to attain supported cobalt catalysts. It was found that the non-noble metal based 10 wt.% $Co/CeZrO_4$ is an efficient catalyst to achieve ethanol conversion of 100% and hydrogen yield of 82% (4.9 mol H_2/mol ethanol) at 450 °C, which is superior to 0.5 wt.% Rh/Al_2O_3. The pre-reduction process is required to activate supported cobalt catalysts for high H_2 yield of ethanol steam reforming. In addition, support effect is found significant for cobalt during ethanol steam reforming. 10% Co/CeO_2 gave high H_2 selectivity while suffered low conversion due to the poor thermal stability. In contrast to CeO_2, 10 wt.% Co/ZrO_2 achieved high conversion while suffered lower H_2 yield due to the production of methane. The synergistic effect of ZrO_2 and CeO_2 to promote high ethanol conversion while suppress methanation was observed when $CeZrO_4$ was used as a support for cobalt. This synergistic effect of $CeZrO_4$ support leads to a high hydrogen yield at low temperature for 10 wt.% $Co/CeZrO_4$ catalyst. Under the high weight hourly space velocity (WHSV) of ethanol (2.5 h^{-1}), the hydrogen yield over 10 wt.% $Co/CeZrO_4$ was found to gradually decrease to 70% of its initial value in 6 h possibly due to the coke formation on the catalyst.

Keywords Hydrogen production · Ethanol steam reforming · Cobalt · Cerium-zirconium oxide

1 Introduction

Economic and environmental concerns make hydrogen the most favorable fuel for proton-exchange membrane fuel cells (PEMFCs) because hydrogen fuel cells provide high efficiency without greenhouse gas emission as water is its only byproduct [1, 2]. Liquid hydrocarbon fuels are promising hydrogen carriers because they have a high specific energy density and can be easily stored in a small fuel tank at ambient temperature and pressure. Furthermore, by shifting the hydrogen source from limited fossil fuels to biomass fuels such as bioethanol, renewable hydrogen can be produced in a CO_2 neutral environment, therefore reduce the impact to the global warming [3, 4]. Hydrogen production via catalytic steam reforming is a cost effective and an efficient process [5, 6]. Steam reforming of bioethanol is particularly interesting because the fermentation broth typically contains diluted ethanol of 12% by volume and can be directly subjected to the reformer without additional steam to produce hydrogen. Since the steam reforming can be activated at mid-temperature range (350–500 °C), the steam reformer can be directly connected to down stream high-temperature water-gas shift reactor (which typically operates in the close temperature range) without additional heat exchanger [7, 8]. When using stoichiometric feedstocks, the overall reaction for ethanol steam reforming is shown in Eq. 1.

S. S.-Y. Lin · S. Y. Ha (✉)
Department of Chemical Engineering, Washington State University, P.O. Box 642710, Pullman, WA 99164-2710, USA
e-mail: suha@wsu.edu

D. H. Kim
Pacific Northwest National Laboratory, Institute for Interfacial Catalysis, P.O. Box 999, Richland, WA 99354, USA

$$C_2H_5OH + 3H_2O \rightarrow 6H_2 + 2CO_2;\ \Delta H^0_{298} = +347.4\ \text{kJ/mol} \quad (1)$$

Depending on the type of catalysts and reaction conditions used, hydrogen selectivity is found significantly governed by complicated reaction mechanisms including decomposition, dehydration, dehydrogenation, methanation, water-gas shift reaction, Boudart reaction, and coke formation [9, 10].

The catalyst development for ethanol steam reforming is on its early stage since no commercial catalyst available to date to extract hydrogen from ethanol. Yet much attention has been paid in recent years to progress this field by using various supported catalyst systems [11]. Supported rhodium catalysts have been extensively studied for ethanol steam reforming [12–17]. Rhodium is known as an efficient catalytic metal to break carbon–carbon bond of possible intermediates such as acetaldehyde and oxametallacycle during ethanol steam reforming [18–21]. However, the extremely high cost of rhodium, even compared with other noble metals such as platinum, limits large scale applications. Alternatively, inexpensive base metals such as nickel, copper, and cobalt have shown to possess similar activity toward ethanol steam reforming if the supporting system being carefully chosen [22–24]. Cobalt-based catalysts have been reported to possess noble-metal like activity for the cleavage of carbon–carbon bond at temperature around 400 °C to produce hydrogen from ethanol steam reforming. Several support materials have been used for cobalt including Al_2O_3, MgO, ZnO, SiO_2, and ZrO_2 [25–29]. The effect of preparation method and pretreatment conditions over supported cobalt catalysts are the major issues being concerned for ethanol steam reforming. The nature of active species in cobalt-based catalysts is currently under investigations and is highly associated with the dispersion of cobalt precursor and the reducibility of calcined cobalt oxides on the surface of the chosen support. Moreover, catalyst-support interactions might also play an important role in modifying the catalytic activity and altering the reaction mechanisms.

Cerium oxide (CeO_2) has been used as a major additive to fuel cell electrolyte because it has high oxygen ion conductivity at operating temperatures (500–800 °C) for solid oxide fuel cells (SOFCs) [30]. In catalysis, however, CeO_2 is known to be an effective promoter used in applications such as three-way catalysis (TWC) due to its high oxygen storage capacity (OSC). During the reaction, highly mobile lattice oxygen of CeO_2 rapidly changes the state of oxygen vacancies that allows CeO_2 to act as a catalytic oxygen buffer to enhance the reducibility of the supported metals [31]. Moreover, the oxygen mobility that gives redox characteristic of CeO_2 could promote reaction in a specific pathway under the oxygen-rich environment such as ethanol steam reforming. The insertion of ZrO_2 into CeO_2 structure has been reported to enhance the redox properties as well as the thermal stability of CeO_2 [30, 32]. Consequently, CeO_2–ZrO_2, or $CeZrO_4$ has shown great potential as a catalyst support for reforming catalysis due to its thermal stability and redox properties. There are few reports using $CeZrO_4$ support for catalytic ethanol steam reforming. Roh et al. [13, 14] used $CeZrO_4$ to support rhodium for ethanol steam reforming and obtained a high H_2 yield at 450 °C. This high catalytic activity was possibly attributed to the mobile oxygen provided by support, which suppress methane formation. They also reported that the addition of potassium has a beneficial effect on catalyst activity and stability. Biswas et al. used 30 wt.% Ni/$Ce_{0.74}Zr_{0.26}O_2$ for ethanol steam reforming and suggested that the high oxygen storage capacity of cubic $Ce_{0.74}Zr_{0.26}O_2$ helps to improve the catalytic activity [33]. Vargas et al. prepared a fluorite type Ce–Zr–Co mixed oxide by a pseudo sol–gel method for bioethanol steam reforming [34]. They have found that cobalt was either inserted in the fluorite lattice or well dispersed since only one cubic structure of $CeZrO_4$ detected by XRD. They also observed that partially reduced Co^0/Ce–Zr–Co mixed oxide showed high hydrogen yield but deactivated at higher reaction temperature, in which the cobalt has undergone further reduction and weakened the metal-support interactions. There is no published work using $CeZrO_4$ to support cobalt for ethanol steam reforming. In addition, very few comparative studies were conducted using $CeZrO_4$ support and have shown little understanding of support effect in reforming catalysis. Therefore, in this study, three supported cobalt catalysts based on CeO_2, ZrO_2, and $CeZrO_4$ were prepared and characterized for ethanol steam reforming. Catalyst performance tests were conducted under various conditions to investigate the effect of support on H_2 production rate.

2 Experimental

2.1 Catalyst Preparation and Testing

Three commercial supports, zirconium oxide (ZrO_2, Alfa Aesar), cerium oxide (CeO_2, Alfa Aesar), and cerium-zirconium oxide ($CeZrO_4$, Sigma-Aldrich,) were used for preparing supported cobalt oxides by the incipient wetness method. This was done by impregnating an cobalt nitrate precursor ($Co(NO_3)_2 \cdot 6H_2O$, Alfa Aesar) on the supports, followed by calcination in air at 500 °C for 4 h. All supported cobalt catalysts were prepared to have a cobalt loading of 10 wt.%, which are denoted as 10% Co/CeO_2, 10% Co/ZrO_2, and 10% Co/$CeZrO_4$. The supported rhodium catalyst (0.5% wt. on alumina) used in this study was

purchased from Alfa Aesar. All the reforming experiments were carried out in an 8 mm ID quartz plug-flow reactor inside a WATLOW temperature-controlled furnace at atmospheric pressure. The total amount of the catalyst charged (cobalt plus supports) was approximately 500 mg. Gas flows were controlled by Brooks Mass Flow Controllers (Model 5850E).

In situ H_2 reduction was carried out for all supported catalysts and $CeZrO_4$ support before their activity tests were performed. Typically, supported cobalt catalysts and $CeZrO_4$ support were reduced from 25 °C to 677 °C (10.87 °C/min) under 50 sccm H_2 and held for 1 h at 677 °C. Supported rhodium catalyst was reduced at 350 °C under 50 sccm H_2 for 30 min. Ethanol and water were injected into the reactor by two syringe pumps and vaporized in a pre-heater containing a silicone carbide bed with a 10 sccm helium carrier gas. Ethanol was fed with weight hourly space velocity (WHSV) of 0.63 h^{-1} and a steam-to-carbon ratio (S/C) of 4 was used, unless specified otherwise. Prior to the analysis of the gas compositions, the product stream was passed through a condenser to remove unconverted liquid hydrocarbons and water. The effluent composition was analyzed by an SRI gas chromatograph equipped with a thermal conductivity detector (TCD), molecular sieve 13X, and hayesep D columns capable of separating and measuring H_2, CH_4, CO, CO_2, C_2H_6, and C_2H_4 of the exit gas.

The performance of the catalysts was analyzed in terms of ethanol conversion and hydrogen yield. The ethanol conversion was defined as the mole ratio of the gaseous carbon compounds (CH_4, C_2H_6, C_2H_4, CO, and CO_2) in the product stream to the feed ethanol. The hydrogen yield was defined as the mole ratio of the produced hydrogen to the theoretical amount of hydrogen that could be produced from the feed ethanol (6 mol H_2/ mol ethanol). The mole fraction of the product stream was used to describe the gaseous product composition in this study. This mole fraction of the product stream was defined as the mole ratio of the specific product to the total gaseous products; e.g.

$$H_2 \text{ (mole fraction)} = H_2/(H_2 + CH_4 + C_2H_6 + C_2H_4 + CO + CO_2).$$

2.2 Catalyst Characterization

Catalyst characterization consisted of Brunauer-Emmett-Teller (BET) surface area measurements (Coulter SA-3100 automated characterization machine), thermogravimetric analysis (TGA) and X-ray diffractometry. The X-ray diffraction data was collected on a Philips X'Pert MPD (Model PW3040/00) instrument with a Xe-filled proportional counter detector. The X-ray source was a long fine-focus and sealed ceramic X-ray tube (Cu anode) operated at 40 kV and 50 mA (2000 W). TGA experiments and derivative thermogravimetric curves (DTG) were carried out using a NETZSCH STA 409 PC instrument. The mass change of the sample was studied under the same temperature-programmed procedure of the in situ H_2 reduction. Approximately 20 mg of sample was thermally treated from 25 °C to 677 °C under 20 sccm carrier gas (50% H_2/He) with a heating rate of 10.87 °C/min and held for 1 hour at 677 °C.

3 Results and Discussion

3.1 Characterization of Supported Cobalt Catalysts

The BET surface areas of the supports and the supported catalysts were summarized in Table 1. Among the supports used, $CeZrO_4$ support gives the highest surface areas for supporting cobalt oxide after calcination at 500 °C, as well as for supporting metallic cobalt after H_2 reduction at 677 °C. In Fig. 1 XRD spectra shows the evolution of the crystalline structure of 10% Co/$CeZrO_4$ sample as it underwent the calcinations and reduction/reforming processes. The XRD spectra for 10% Co/$CeZrO_4$ sample after H_2 reduction process followed by reforming operation for 1 h is denoted as a spent sample in Fig. 1. As expected, the peaks of cubic cobalt oxides (Co_3O_4) indicate that cobalt precursor impregnated on cubic $CeZrO_4$ support and it is oxidized during the calcination process. The formation of Co_3O_4 was also found on cubic CeO_2 and monoclinic ZrO_2 supports as can be seen from the calcined samples of 10% Co/CeO_2 and 10% Co/ZrO_2. In addition, XRD spectra shows that Co_3O_4 was further transformed to metallic cobalt on $CeZrO_4$ (spent sample) as the supported cobalt catalyst reduced in H_2 and used for ethanol steam reforming in the condition with no catalyst deactivation. No peaks corresponding to cobalt oxide found in the spent 10% Co/$CeZrO_4$ indicating that supported cobalt oxide was fully transformed to metallic cobalt in H_2 reduction

Table 1 Brunauer–Emmett–Teller surface area of the supports and the supported catalysts

Catalyst/Support	BET surface area (m^2/g)		
	Support	Calcined	Reduced
ZrO_2	106	–	–
10% Co/ZrO_2	–	57	34
CeO_2	80	–	–
10% Co/CeO_2		32	14
$CeZrO_4$	158	–	–
10% Co/$CeZrO_4$	–	77	38

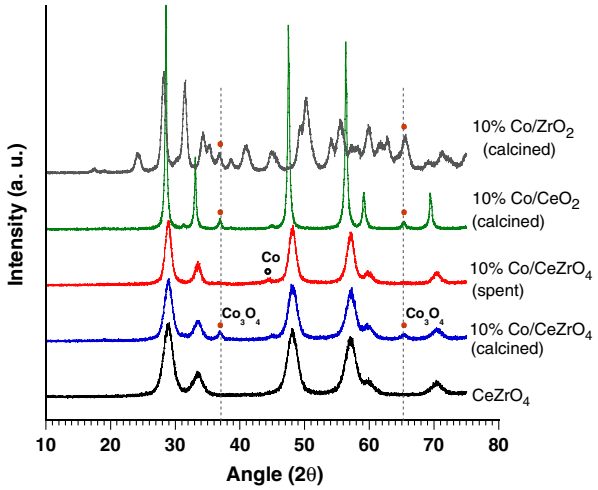

Fig. 1 XRD spectra of $CeZrO_4$ support, calcined 10% $Co/CeZrO_4$, spent 10% $Co/CeZrO_4$, calcined 10% Co/CeO_2, and calcined 10% Co/ZrO_2

process, and maintained its metallic state in the ethanol steam reforming condition.

Figure 2 shows four DTG curves of support and the supported cobalt catalysts during the temperature-programmed H_2 reduction. The peaks shown in the temperature region below 100 °C for all samples are due to the removal of physisorbed water from the catalyst surfaces. As temperature increased, two major weight loss peaks occurred at temperature ranges of 280–310 °C and 360–440 °C for each supported cobalt catalyst. These two major weight loss peaks indicate the composition changes of cobalt oxide (Co_3O_4). Under H_2 environment, Co_3O_4 is known to be readily reduced to CoO and metallic cobalt in these temperature regions ($Co_3O_4 \rightarrow CoO \rightarrow Co$) [35]. Moreover, the degree of reduction is found influenced by the reducing environment such as composition of carrier gas and

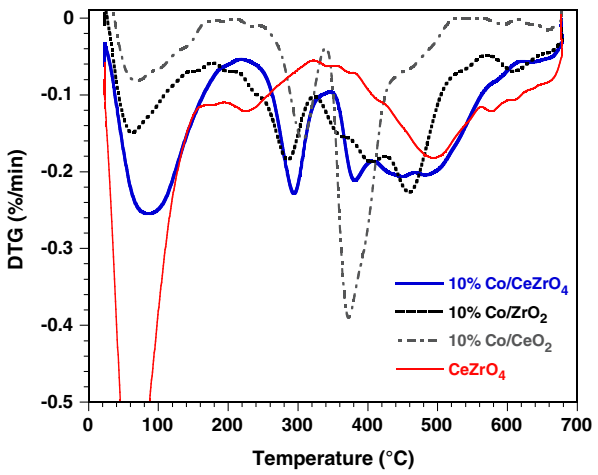

Fig. 2 DTG profiles of $CeZrO_4$ support and supported cobalt catalysts under H_2 temperature-programmed reduction

supporting material for cobalt. We speculate that the first peaks for three supported cobalt catalysts in the temperature range between 280 and 310 °C account for the first reduction process of cobalt ($Co^{3+} \rightarrow Co^{2+}$), while the second peaks in the temperature range between 360 and 440 °C accounts for the second reduction process of cobalt ($Co^{2+} \rightarrow Co^0$). According to Fig. 2, it seems that the second reduction peaks for both 10% $Co/CeZrO_4$ and 10% Co/ZrO_4 are splitted into two peaks, while 10% Co/CeO_2 shows a single second reduction peak at 370 °C. In addition, Fig. 2 indicates that there are peak shifts of both the first and second reduction processes for three supported cobalt catalysts. These peak splits and shifts suggest that the reduction behavior of metallic cobalt might have strong interaction with the support surfaces. Furthermore, the peak around 500 °C for $CeZrO_4$ suggests that the support was reduced under H_2. The same peak is observed for 10% $Co/CeZrO_4$ with a little down shift and it suggests a complicated reduction reaction occurred between surfaces of metallic cobalt, cobalt oxide and $CeZrO_4$ support. This reduction behavior might significantly modify the catalytic properties of 10% $Co/CeZrO_4$ and result in a high H_2 selectivity as pre-reduction proceeded. The detailed investigation for the correlation between the catalyst reduction process and the catalytic properties is needed. In situ XRD measurement which can dynamically measure the crystalline structure of cobalt and $CeZrO_4$ during the various reduction processes is currently being carried out in our lab, and it is expected to provide insightful information of catalyst-support interactions toward catalytic properties.

3.2 Activity Test of Supported Cobalt Catalysts

The activity tests were conducted under various operating conditions to examine the catalytic activity of the supported cobalt catalysts toward ethanol steam reforming. Figure 3 shows the effect of reaction temperature on hydrogen yield for the cobalt supported on $CeZrO_4$ with two different loadings (1% and 10% $Co/CeZrO_4$) and the rhodium supported on Al_2O_3 (0.5% Rh/Al_2O_3). Under a weight hourly space velocity of 0.63 h^{-1} and a steam-to-carbon ratio of four, 1% $Co/CeZrO_4$ gave comparable H_2 yield comparing to 0.5% Rh/Al_2O_3. The H_2 yield over both supported catalysts was close to the equilibrium value in the course of reaction temperature. However, when loading of cobalt increased from 1% to 10% on $CeZrO_4$, the H_2 yield exceeded equilibrium and reached at a maximum value at 450 °C (4.9 mol H_2/mol ethanol). The result demonstrated that the exceptional high activity for ethanol steam reforming can be obtained by increasing the loading of inexpensive cobalt on $CeZrO_4$ support at lower temperature as compared with equilibrium. This was further

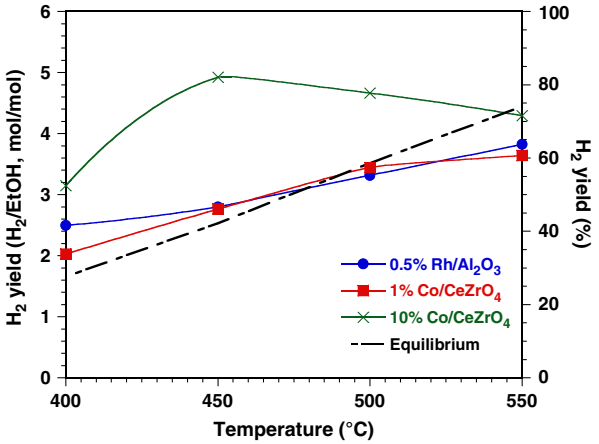

Fig. 3 The hydrogen yield of ethanol steam reforming over supported rhodium and cobalt catalysts. S/C ratio is four and the weight hourly space velocity (WHSV) of ethanol is 0.63 h^{-1}

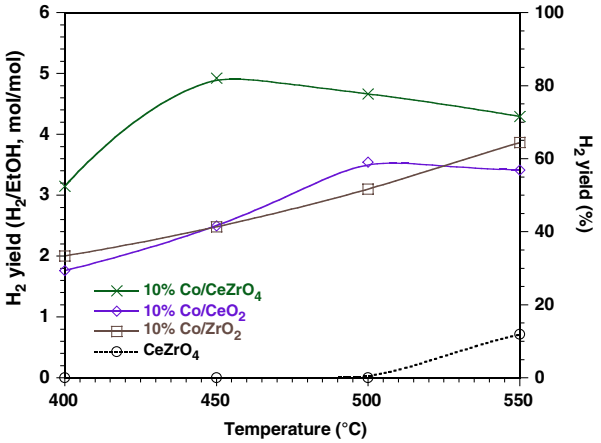

Fig. 5 The hydrogen yield of ethanol steam reforming over $CeZrO_4$ support and supported cobalt catalysts. S/C ratio is four and the weight hourly space velocity (WHSV) of ethanol is 0.63 h^{-1}

verified in Fig. 4 in which 10% Co/$CeZrO_4$ shown the highest hydrogen production rate at 450 °C as the ethanol feeding rate increased. Figure 5 shows the H_2 yield over $CeZrO_4$ support and cobalt supported on CeO_2, ZrO_2, and $CeZrO_4$. As can be seen the effect of support on H_2 yield is significant. 10% Co/$CeZrO_4$ gave the highest H_2 yield suggests that CeO_2–ZrO_2 combination exhibited interesting supporting effect for cobalt during ethanol steam reforming. The enhancement toward H_2 production must arise from the interactions between $CeZrO_4$ and cobalt since nearly no hydrogen produced over the $CeZrO_4$ support. In addition to the high H_2 yield, the ethanol conversion over 10% Co/$CeZrO_4$ has shown to reach the equilibrium value at 450 °C as it is shown in Fig. 6. In comparison with Co/$CeZrO_4$ catalyst, higher operation temperature was required to reach the equilibrium conversion when using either CeO_2 or ZrO_2 to support cobalt. It is noticed that although $CeZrO_4$ attained fairly high conversion without supporting cobalt, no hydrogen was produced until temperature reached 550 °C as mentioned in Fig. 5. The product composition of ethanol steam reforming over $CeZrO_4$ and supported cobalt catalysts at 450 °C are presented in Fig. 7. As can be seen, without supporting cobalt, $CeZrO_4$ converted 60% of ethanol while showed low activity to the cleavage of carbon-carbon bonds and produced hydrogen-contained byproducts such as ethylene. The high selectivity toward ethylene (60%) suggests that dehydration of ethanol was promoted under the reaction conditions over $CeZrO_4$. Moreover, the small portion of ethane in the product stream suggests that there might be a hydrogenation followed by the formation of ethylene. However, the reaction pathway can be diverted when cobalt was supported on $CeZrO_4$. With 100% of ethanol

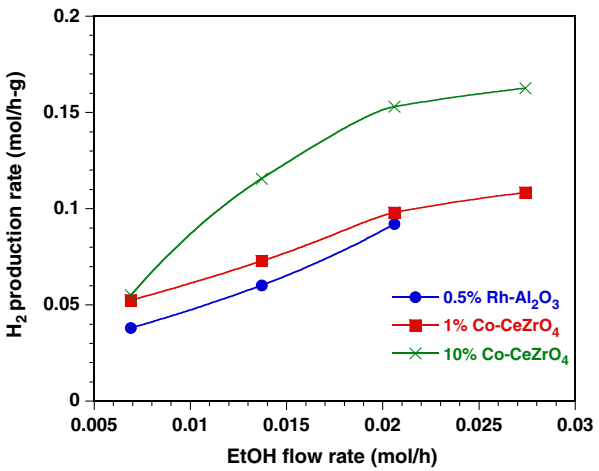

Fig. 4 The hydrogen production rate of ethanol steam reforming over supported rhodium and cobalt catalysts at 450 °C. S/C ratio is four

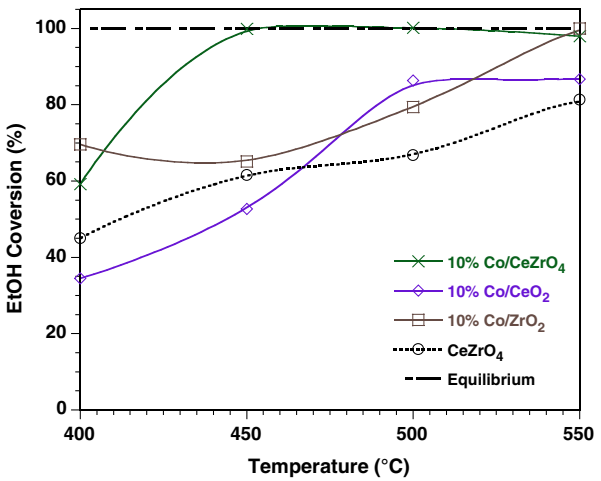

Fig. 6 The ethanol conversion of ethanol steam reforming over $CeZrO_4$ support and supported cobalt catalysts. S/C ratio is four and the weight hourly space velocity (WHSV) of ethanol is 0.63 h^{-1}

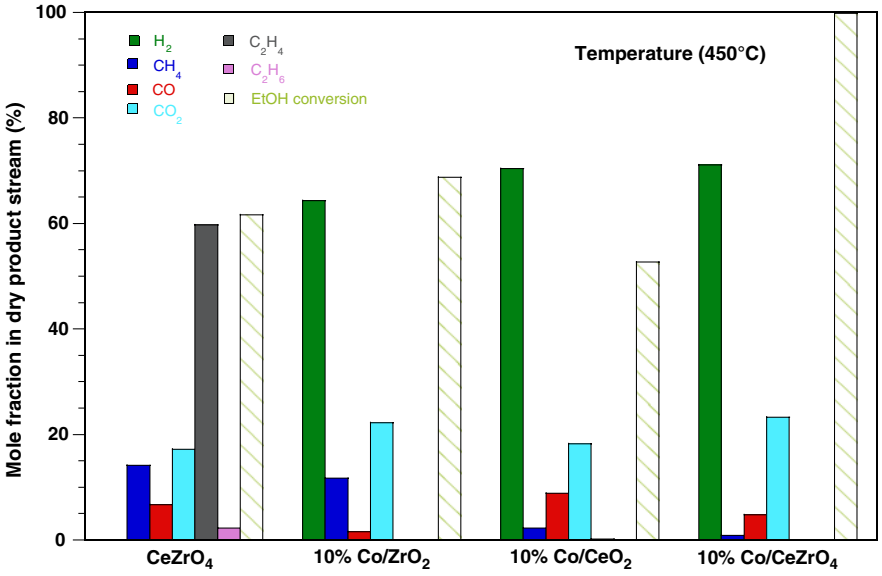

Fig. 7 The product composition of ethanol steam reforming over $CeZrO_4$ support and supported cobalt catalysts. S/C ratio is four and the weight hourly space velocity (WHSV) of ethanol is 0.63 h^{-1}

being converted, very low hydrogen-contained byproduct (0.85% methane) was produced over 10% $Co/CeZrO_4$ that lead to a high selectivity toward H_2 (71%). The effect of support on product distribution is also shown as ethanol conversion and H_2 selectivity were compared over three supported cobalt catalysts in Fig. 7. As compared with 10% $Co/CeZrO_4$, lower conversion was observed for other two supported catalyst systems and might be partially attributed to the effect of lower surface area for 10% Co/CeO_2. 10% Co/ZrO_2 on the other hand, possessed similar surface area to that of 10% $Co/CeZrO_4$, but required higher reaction temperature to achieve the equilibrium conversion. Methane was the only hydrogen-contained byproduct in all supported cobalt catalysts, which demonstrated cobalt's role in the cleavage of carbon–carbon bond of ethanol. Nevertheless, the effect of support could be prominent in the subsequent reactions such as methanation and water-gas shift reaction. The result shows that less H_2 selectivity by 10% Co/ZrO_2 is due to the higher methane production (12%).

The results of the long-term catalytic activity test for 10% $Co/CeZrO_4$ are shown in Fig. 8. Under the high weight hourly space velocity of ethanol (2.5 h^{-1}) and a steam-to-carbon ratio of ten, the hydrogen yield that was found to gradually decrease to 70% of its initial value in 6 h indicates catalyst deactivation. Although XRD spectrum taken from spent sample showed no further oxidation of cobalt occurred during ethanol steam reforming, there are other possibilities such as sintering and coking that can lead to the observed catalyst deactivation. The deactivation is likely due to the coke build up on the surface of catalyst during the carbon–carbon cleavage and possibly from Boudart reaction ($2CO \leftrightarrow CO_2 + C$). Our preliminary results have shown that the activity of deactivated 10% $Co/CeZrO_4$ can be largely recovered under H_2 treatment at 500 °C. The regeneration with H_2 produced methane which detected by GC indicating the surface carboneous residue due to the coking converted by H_2 and gave rise to CH_4.

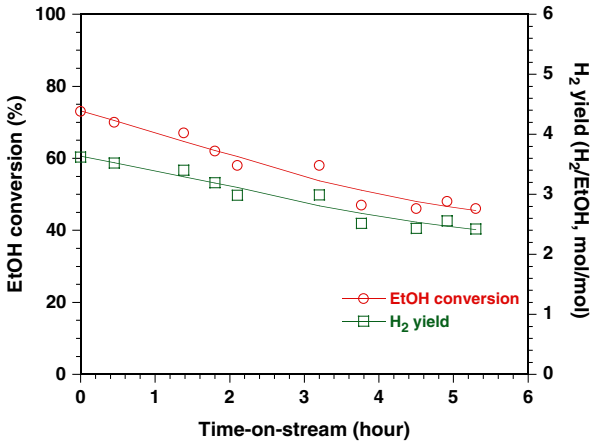

Fig. 8 Time-on-stream testing of 10% $Co/CeZrO_4$ for ethanol steam reforming at 450 °C. S/C ratio is ten and the weight hourly space velocity (WHSV) of ethanol is 2.52 h^{-1}

4 Conclusions

Cobalt supported on $CeZrO_4$ has shown superior activity to produce H_2 via ethanol steam reforming. At 450 °C, equilibrium conversion of ethanol (100%) and hydrogen yield of 82% (4.9 mol H_2/mol ethanol converted) were achieved by 10 wt.% $Co/CeZrO_4$, which is superior to 0.5 wt % Rh/Al_2O_3. The support effect on both activity and H_2 selectivity was observed when cobalt supported on CeO_2, ZrO_2, and $CeZrO_4$. Based on the results, we used

$CeZrO_4$ to support cobalt which gives the synergistic effect of CeO_2 and ZrO_2 supports to promote a high ethanol conversion while suppress methanation. Thus, 10 wt.% $Co/CeZrO_4$ provides a high hydrogen yield at low temperature. The activity of 10 wt.% $Co/CeZrO_4$ catalyst was found gradually decreased in the time-on-stream test, which is possibly due to the coke formation on the catalyst because the regeneration was achievable under the H_2 thermal treatment. In order to improve the current catalyst system with an even greater hydrogen yield and higher stability, further investigation including in situ XRD and in situ FTIR will be needed to attain a better understanding of catalyst-support interactions toward the related catalytic properties.

Acknowledgements The authors would like to acknowledge the O. H. Reaugh Fund for the support of this work.

References

1. Cropper MAJ, Geiger S, Jollie DM (2004) J Power Sources 131:57–61
2. Jacobson MZ, Colella WG, Golden DM (2005) Science 308:1901–1905
3. Demirbas A (2007) Prog Energy Combust 33:1–18
4. Hamelinck CN, Faaij APC (2006) Energy Policy 34:3268–3283
5. Rostrup-Nielsen JR, Sehested J, Norskov JK (2002) Adv Catal 47:65–139
6. Song CS (2002) Catal Today 77:17–49
7. Farrauto RJ, Liu Y, Ruettinger W, Ilinich O, Shore L, Giroux T (2007) Catal Rev-Sci Eng 49:141–196
8. Bartholomew CH, Farrauto RJ (2006) Fundamentals of industrial catalytic processes, 2nd edn. Wiley, Hoboken
9. Vaidya PD, Rodrigues AE (2006) Chem Eng J 117:39–49
10. Haryanto A, Fernando S, Murali N, Adhikari S (2005) Energy Fuel 19:2098–2106
11. Duan S, Senkan S (2005) Ind Eng Chem Res 44:6381–6386
12. Montini T, De Rogatis L, Gombac V, Fornasiero P, Graziani M (2007) Appl Catal B Environ 71:125–134
13. Roh HS, Wang Y, King DL, Platon A, Chin YH (2006) Catal Lett 108:15–19
14. Roh HS, Platon A, Wang Y, King DL (2006) Catal Lett 110:1–6
15. Diagne C, Idriss H, Kiennemann A (2002) Catal Commun 3:565–571
16. Breen JP, Burch R, Coleman HM (2002) Appl Catal B Environ 39:65–74
17. Cavallaro S (2000) Energy Fuel 14:1195–1199
18. Idriss H (2004) Platinum Metals Rev 48:105–115
19. Chen HL, Liu SH, Ho JJ (2006) J Phys Chem B 110:14816–14823
20. Mavrikakis M, Barteau MA (1998) J Mol Catal A Chem 131:135–147
21. Mavrikakis M, Doren DJ, Barteau MA (1998) J Phys Chem B 102:394–399
22. Dasi NK, Dalai AK, Ranganathan R (2007) Can J Chem Eng 85:92–100
23. Carrero A, Calles JA, Vizcaino AJ (2007) Appl Catal A Gen 327:82–94
24. Homs N, Llorca J, de la Piscina PR (2006) Catal Today 116:361–366
25. Song H, Zhang L, Ozkan US (2007) Green Chem 9:686–694
26. Sahoo DR, Vajpai S, Patel S, Pant KK (2007) Chem Eng J 125:139–147
27. Batista MS, Santos RKS, Assaf EM, Assaf JM, Ticianelli EA (2004) J Power Sources 134:27–32
28. Llorca J, Homs N, Sales J, de la Piscina PR (2002) J Catal 209:306–317
29. Haga F, Nakajima T, Miya H, Mishima S (1997) Catal Lett 48:223–227
30. Ahn KY, He HP, Vohs JM, Gorte RJ (2005) Electrochem Solid State Lett 8:A414–A417
31. Campbell CT, Peden CHF (2005) Science 309:713–714
32. Kozlov AI, Kim DH, Yezerets A, Andersen P, Kung HH, Kung MC (2002) J Catal 209:417–426
33. Biswas P, Kunzru D (2007) Int J Hydrogen Energy 32:969–980
34. Vargas JC, Libs S, Roger AC, Kiennemann A (2005) Catal Today 107–108:417–425
35. Jones A, McNicol BD (1986) Temperature-programmed reduction for solid materials characterization. M Dekker, New York